AGU PUBLICATIONS

Geophysical Research Letters

RESEARCH LETTER
10.1002/2015GL064823

Key Points:
- The first derivation of freeboard using Ka band radar altimetry
- The radar penetration into the snow pack depends on the operating frequency of the instrument
- CryoSat-2 does not always range to the ice/snow interface over multiyear sea ice in March

Supporting Information:
- Supporting Information S1, Figures S1–S3

Correspondence to:
T. W. K. Armitage,
t.armitage@ucl.ac.uk

Citation:
Armitage, T. W. K., and A. L. Ridout (2015), Arctic sea ice freeboard from AltiKa and comparison with CryoSat-2 and Operation IceBridge, *Geophys. Res. Lett.*, *42*, doi:10.1002/2015GL064823.

Received 4 JUN 2015
Accepted 31 JUL 2015
Accepted article online 3 AUG 2015

Arctic sea ice freeboard from AltiKa and comparison with CryoSat-2 and Operation IceBridge

Thomas W. K. Armitage[1] **and Andy L. Ridout**[1]

[1]Centre for Polar Observation and Modelling, University College London, London, UK

Abstract Satellite radar altimeters have improved our knowledge of Arctic sea ice thickness over the past decade. The main sources of uncertainty in sea ice thickness retrievals are associated with inadequate knowledge of the snow layer depth and the radar interaction with the snow pack. Here we adapt a method of deriving sea ice freeboard from CryoSat-2 to data from the AltiKa Ka band radar altimeter over the 2013–14 Arctic sea ice growth season. AltiKa measures basin-averaged freeboards between 4.4 cm and 6.9 cm larger than CryoSat-2 in October and March, respectively. Using airborne laser and radar measurements from spring 2013 and 2014, we estimate the effective scattering horizon for each sensor. While CryoSat-2 echoes penetrate to the ice surface over first-year ice and penetrate the majority (82 ± 3%) of the snow layer over multiyear ice, AltiKa echoes are scattered from roughly the midpoint (46 ± 5%) of the snow layer over both ice types.

1. Introduction

An important development in sea ice research over the past decade has been the utility of satellite radar and laser altimeter data for estimating basin-scale Arctic sea ice thickness [*Laxon et al.*, 2003; *Giles et al.*, 2008; *Kwok et al.*, 2009; *Laxon et al.*, 2013; *Meier et al.*, 2014], making it possible to estimate the total Arctic sea ice volume. The total ice volume is an important climate parameter as sea ice stores and releases latent heat and fresh water as it grows and shrinks in volume over the course of a season, affecting the high-latitude energy and oceanic salt budgets. For Ku band radar altimeters (13.6 GHz central frequency) operating over sea ice it is often assumed that the ice-snow interface is the dominant scattering horizon [*Laxon et al.*, 2003; *Giles and Hvidegaard*, 2006; *Giles et al.*, 2007, 2008; *Laxon et al.*, 2013; *Kurtz et al.*, 2014; *Ricker et al.*, 2014]. The freeboard to thickness conversion then depends on how much the ice-snow interface is depressed relative to the sea surface height by the weight (i.e., depth and density) of the overlying snow layer which is typically taken from the climatology of *Warren et al.* [1999], as well as the density of the ocean water and sea ice. The ice thickness uncertainty is dominated by the lack of knowledge of the instantaneous snow depth (~50%) and the freeboard measurement error (~40%), with smaller contributions from the uncertainty of the water, ice, and snow densities [*Giles et al.*, 2007].

In view of results from field campaigns [*Giles and Hvidegaard*, 2006; *Hendricks et al.*, 2010; *Willatt et al.*, 2011; *Willatt*, 2012], *Laxon et al.* [2013] cautioned that there may be residual errors in sea ice thickness estimates due to scattering from the air-snow interface and within the snow pack. *Kwok* [2014] suggests that this may be the case for airborne Ku band radar, particularly where there is a thicker snow layer present, but the extent to which satellite radar altimeters are affected by snow surface and volume scattering is currently unknown. However, it is known that radar backscattering properties of the snow on sea ice are very sensitive even to small amounts of liquid water content and the presence of salt (brine) or icy layers [*Ulaby et al.*, 1986; *Willatt*, 2012], so the radar freeboard (the freeboard measured by a radar altimeter) has been introduced as a separate quantity to the sea ice freeboard (the elevation of the ice surface above local sea level) [*Ricker et al.*, 2014]. In this letter, we estimate radar freeboard using Ka band radar altimeter data (35.75 GHz central frequency) for the first time. Then through comparison with Ku band altimetry and airborne laser and radar data, we estimate the effective radar penetration of the snow pack at both Ka and Ku band.

2. Data and Methods

We use data from two polar-orbitting satellite radar altimeters: the AltiKa instrument on board the Satellite for ARgos and ALtiKa (SARAL) and the Synthetic Aperture Radar (SAR) Interferometric Radar Altimeter (SIRAL) on

board the CryoSat-2 (CS2) satellite. SARAL/AltiKa (herein referred to as AltiKa) is a joint mission between the French space agency (Centre National d'Études Spatiales) and the Indian Space Research Organisation and became operational on 14 March 2013 [*Bronner*, 2013]. AltiKa occupies the same orbit as the Envisat satellite, giving coverage to 81.5°N/S but operates at a central frequency of 35.75 GHz with 500 MHz bandwidth, making it the first space-borne Ka band radar altimeter. AltiKa should offer improved performance over sea ice relative to pulse-limited Ku band altimeters (e.g., ERS, Envisat) as it will be less sensitive to waveform contamination by bright off nadir features. This is for two main reasons: first, AltiKa has a pulse-limited footprint of ∼1.4 km, compared to ∼1.7 km for pulse-limited Ku band altimeters, and second, with a beam width of 0.6° compared to 1.3° at Ku band, AltiKa is close to being a beam-limited altimeter, so the waveform power is attenuated much more quickly after a sharper peak. In effect, the surface area illuminated is much smaller at Ka band than at Ku band, and power received from higher incidence angles is more strongly attenuated. In contrast to AltiKa, CS2 was specifically designed to measure the Earth's terrestrial and marine ice sheets and occupies a highly inclined orbit giving coverage up to 88°N/S [*Wingham et al.*, 2006]. Over sea ice, along track SAR processing gives SIRAL an along/across track footprint of ∼0.3/1.7 km, allowing sampling of smaller ice floes and reducing data contamination due to bright off nadir features.

To estimate radar freeboard from AltiKa, we make use of the Sensor Geophysical Data Record which contains all of the 40 Hz radar echo waveforms. We adapt the algorithm developed by *Laxon* [1994] for ERS measurements which has since been employed to determine sea ice thickness from CS2 measurements [*Laxon et al.*, 2013] and now forms the basis for the algorithm used by the European Space Agency Sea Ice Climate Change Initiative [*Ridout and Ivanova*, 2012]. The essential step in estimating freeboard from altimeter data is distinguishing between waveforms originating from leads and waveforms originating from sea ice floes. The sea surface height anomaly measured at leads is interpolated underneath sea ice floes, and the floe elevation relative to the interpolated sea surface height is termed the radar freeboard (see supporting information). Note that for the present work, the satellite-derived radar freeboard is not corrected for the slower speed of light propagation in snow to avoid introducing auxiliary snow depth data into the comparison. Monthly radar freeboard estimates from both satellites are then posted onto a 0.8° × 0.2° grid and smoothed using a Gaussian convolution filter with a standard deviation of 50 km.

We also make use of time and space coincident airborne data from NASAs Operation IceBridge (OIB). This allows a comparison between the satellite-derived radar freeboard and the laser freeboard (the elevation of the air-snow interface above local sea level) and snow depth measured by the OIB laser scanner and ultrawideband snow radar. There were 5 OIB sorties over sea ice between 21 and 27 March 2013 and 14 between 12 March and 3 April 2014, and we compare these to satellite data acquired between 14 March and 4 April 2013 and 12 March and 3 April 2014. The OIB Sea Ice Freeboard, Snow Depth, and Thickness Quick Look data are used because the fully consolidated sea ice products are not yet available for these campaigns. The Quick Look products have additional uncertainty compared to the consolidated product; the Quick Look product relies on the surface temperature from the KT19 instrument to identify leads, rather than the full lead identification processing described by *Onana et al.* [2013], as well as the use of near real-time GPS data. For the 2012 OIB campaign, the Quick Look laser freeboard and snow depth have an offset and spread of 1.5 ± 6.0cm and 0.1±2.0 cm, respectively, compared to the consolidated product (documentation available via http://nsidc.org/data/icebridge/evaluation-products.html). It is not currently possible to fully assess the uncertainty on averaged OIB Quick Look snow depths. The snow depth uncertainty in the Quick Look product is set to a constant 5.7 cm [after *Farrell et al.*, 2012] so cannot be treated as random, and *Kurtz et al.* [2013] note that further validation against in situ measurements is required to properly quantify the Quick Look snow depth uncertainty. Nevertheless, OIB data represent a valuable tool for evaluating satellite data; *Laxon et al.* [2013] found less than 5 cm root-mean-square difference between CS2 and OIB-derived sea ice thicknesses.

3. Results

3.1. Comparison Between AltiKa and CryoSat-2

The CS2 and AltiKa radar freeboard and the difference (AltiKa-CS2) are calculated for the 2013–2014 Arctic sea ice growth season (Figure 1). What is immediately clear is the excellent coverage given by CS2, whereas AltiKa does not sample most of the thickest ice to the north of Greenland and the Canadian Arctic Archipelago (CAA). The difference between the AltiKa and CS2 radar freeboard (Figure 1, right) shows that AltiKa consistently retrieves a greater elevation than CS2 over sea ice. Further to this, it can be seen that the difference between AltiKa and CS2 increases over the course of the sea ice growth season and that for a given month

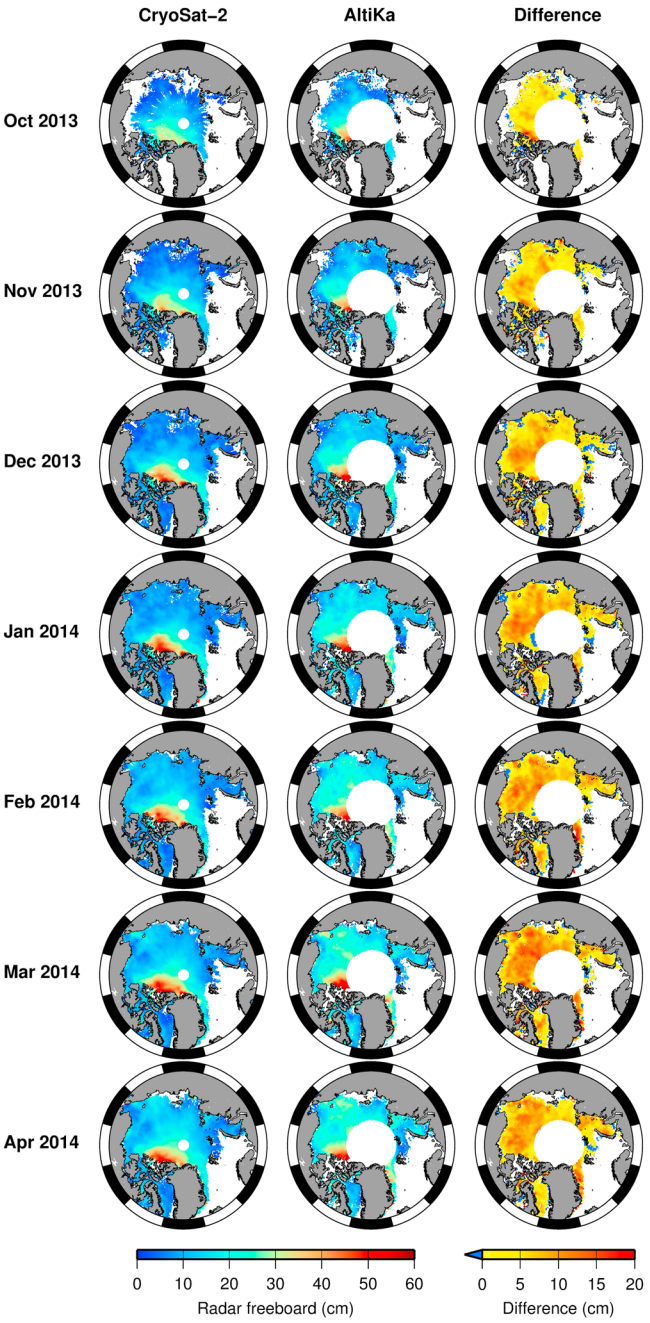

Figure 1. The radar freeboard from (left column) CS2, (middle column) AltiKa, and (right column) the difference (AltiKa-CS2) for the 2013–2014 Arctic sea ice growth season.

the difference varies spatially over the Arctic Basin. Note that the differences in Figure 1 are slightly exaggerated because the radar freeboard has not been corrected for the slower speed of light propagation in snow. Although there are some small areas showing negative differences close to the ice edge, it is likely that this is due to contamination of AltiKa sea ice floe echoes by bright off nadir reflections from leads. This is a known issue for radar altimeters operating over sea ice, particularly pulse-limited instruments: bright off nadir features such as leads can dominate the echo power, causing a later time of arrival and an underestimate of the surface elevation [*Connor et al.*, 2009; *Armitage and Davidson*, 2014].

The area averaged radar freeboard from AltiKa is always larger than for CS2, and the difference between the two sensors changes as the season progresses (Figure 2). In this comparison, the CS2 area averaged freeboard is only calculated up to 81.5°N, the latitudinal limit of the AltiKa data. The mean difference is 4.4 cm in October,

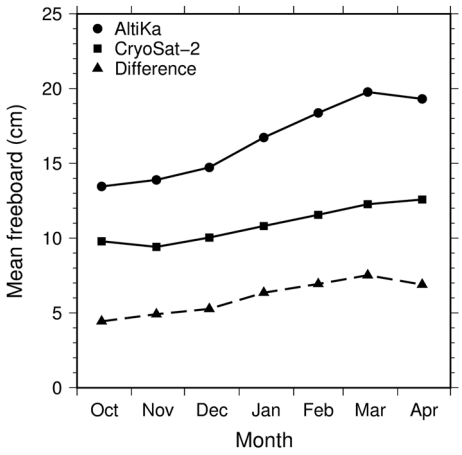

Figure 2. The mean radar freeboard from AltiKa (circles), CS2 (squares), and the difference (AltiKa-CS2, triangles) for the 2013–2014 Arctic sea ice growth season.

growing to 6.9 cm in March before decreasing slightly in April. The CS2 freeboard decreases between October and November 2013 due to a combination of two factors. First, the rapidly expanding seasonal ice zone will decrease the basin-mean freeboard, and second, the thickening of the overlying snow layer in autumn will depress the ice surface relative to sea level [*Warren et al.*, 1999].

3.2. Comparison Between Satellite and Airborne Data

To allow a direct comparison with the satellite-derived radar freeboard, we use the OIB laser freeboard and snow depth to derive radar freeboard, assuming that the ice-snow interface is the dominant scattering horizon and that the radar wave is slowed as it travels through the snow pack. The correction for the slower propagation of radar waves through the snow pack is given by $h_c = h_s(1-c_s/c)$, where h_s is the snow depth, c_s is the speed of light propagation through snow, and c is the speed of light propagation in a vacuum [*Kurtz et al.*, 2014]. Using the value of $c_s/c = 0.781$ quoted by *Kwok* [2014], $h_c \approx 0.2h_s$. The OIB radar freeboard, $F_r^{(OIB)}$, is then

$$F_r^{(OIB)} = F_l - h_s - h_c \approx F_l - 1.2h_s \quad (1)$$

where F_l is the OIB laser freeboard. Finally, as with the satellite-derived radar freeboards, the OIB radar freeboard estimates are gridded on a 0.8° × 0.2° grid. The OIB radar freeboard is correlated with both the laser freeboard ($R = 0.87$) and radar freeboard ($R = 0.49$) suggesting that thicker ice (larger ice freeboard) tends to have a thicker snow layer (Figure 3, left, grey).

The satellite observations are compared with the airborne data by averaging all of the data into 4° × 1° grid cells with grid cells omitted if they contain less than 100 individual freeboard measurements to reduce the impact of speckle noise [after *Laxon et al.*, 2013]. We are then left with 200 grid cells containing both AltiKa and OIB freeboards (Figure 3, left, blue) and 395 grid cells with both CS2 and OIB freeboards (Figure 3, left, orange). There are less AltiKa data points in Figure 3 with larger laser freeboards (>50 cm) because AltiKa does not sample much of the thick ice to the north of Greenland and the CAA. There is a good correlation between both satellite sensors and the OIB radar freeboard ($R = 0.84$ for AltiKa and $R = 0.81$ for CS2).

The comparison between satellite and OIB radar freeboard shows that the elevations retrieved over sea ice are larger at Ka band than at Ku band over all ice thicknesses and snow depths. A larger elevation retrieval

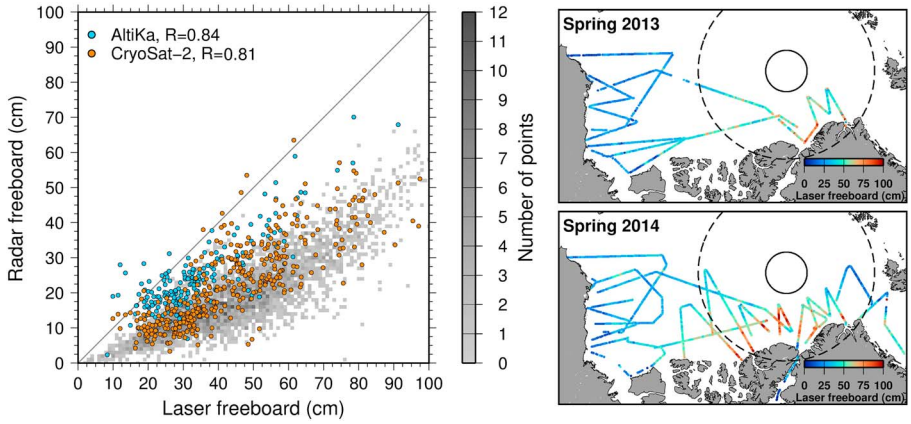

Figure 3. (left) Scatterplot of the radar freeboard from OIB (grey), AltiKa (blue), and CS2 (orange) radar freeboard versus laser freeboard from OIB. OIB flight lines for (top right) spring (March–April) 2013 and (bottom right) spring 2014, colored by the laser-derived snow freeboard. The northern limit of the coverage offered by the two satellites is shown by the solid (CS2) and dashed (AltiKa) circles.

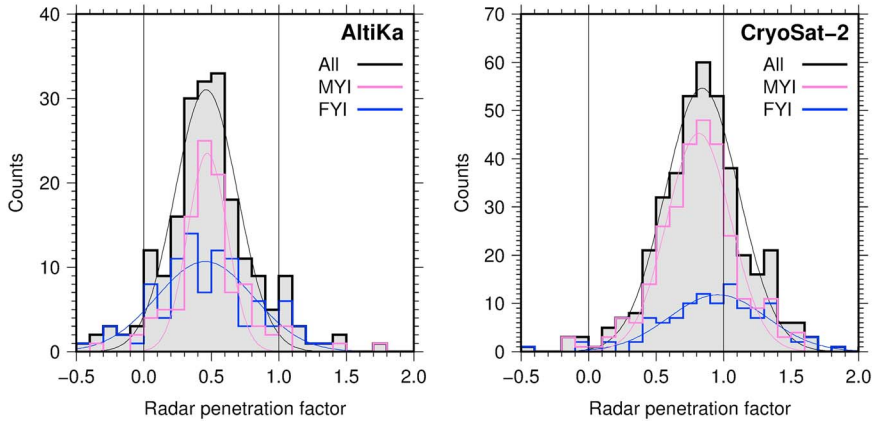

Figure 4. Histograms of the radar penetration factor, f, calculated using equation (2) for (left) AltiKa and (right) CS2. The histograms are further broken down into multiyear ice (MYI) (orchid) and first year ice (FYI) (blue) and the Gaussian fit is overlaid (thin lines).

implies that backscatter from the snow surface and/or volume is stronger at Ka band than at Ku band which shifts dominant scattering horizon toward the satellite [*Kwok*, 2014]. Despite this, the dominant scattering horizon generally lies below the air-snow interface for the whole range of radar freeboard observed by AltiKa. The CS2 radar freeboard generally lies within the range of the observed OIB radar freeboard, supporting the assumption that the ice-snow interface dominates the radar return at Ku band.

4. Discussion

In order to quantify the impact of the difference between the sea ice elevation retrieval from the two satellites, we calculate the radar penetration factor, which we define as:

$$f = \frac{d - \left(F_r^{(\mathrm{sat})} - F_r^{(\mathrm{OIB})}\right)}{d} \tag{2}$$

where $F_r^{(\mathrm{sat})}$ is the satellite-derived radar freeboard, $F_r^{(\mathrm{OIB})}$ is calculated from equation (1), and $d = h_s + h_c$ is the snow depth plus the correction for slower propagation speed of radar waves in snow (see section 2). The radar penetration factor expresses the radar dominant scattering horizon in relation to the snow and ice surfaces; a value of zero indicates that the air-snow interface is the dominant scattering horizon, and a value of one indicates that the ice-snow interface dominates. The radar penetration factor is calculated for all grid cells containing coincident satellite and OIB data. We then discriminate between first year ice (FYI) and multiyear ice (MYI) to investigate whether f depends on the ice age. In general, MYI has a thicker snow layer than FYI [see, e.g., *Newman et al.*, 2014], and we examine the claim of *Kwok* [2014] that the residual error due to snow pack scattering is larger for thicker snow depths.

We fit Gaussian distributions to histograms of the AltiKa and CS2 radar penetration factors (Figure 4) and take the modal radar penetration as the center of the fitted curve (Table 1). The radar penetration factor has a modal value of 0.46 ± 0.05 for Altika and 0.84 ± 0.04 for CS2 for all grid points. The AltiKa radar penetration factor has no apparent dependence on the sea ice type; however, this is not the case for CS2. The Ku band elevation retrieval over FYI is from the ice-snow interface with a radar penetration factor of 0.96 ± 0.08. Over MYI, the Ku band radar penetration factor of 0.82 ± 0.03 indicates that the dominant scattering horizon lies above the ice-snow interface.

Table 1. Modal Radar Penetration Factor for AltiKa and CryoSat-2 for MYI, FYI, and All Data Points[a]

Satellite	MYI	FYI	All
AltiKa	0.47(0.03)	0.45(0.12)	0.46(0.05)
CryoSat-2	0.82(0.03)	0.96(0.08)	0.84(0.04)

[a]The uncertainty, shown in brackets, is the 3 sigma error estimate on the fitted center of the Gaussian curve.

This comparison is only indicative of the relative elevation of the Ka and Ku band dominant scattering horizons within the snow pack, and the following caveats should be considered. There will be discrepancies between the satellite and OIB radar freeboard due to (1) the long period (~20 days) over which the satellite data are averaged in order to have enough coverage to compare with OIB and (2) the different measurement systems and footprint sizes of the satellite and airborne systems. These differences are evident in the spread of data points in the satellite and airborne-derived radar freeboard comparison (Figure 3) and in the spread of the radar penetration histograms, where we even see some values of $f < 0$ and $f > 1$ (Figure 4). The airborne data will be more sensitive to the presence of thinner ice floes that may be missed by the satellites (due to the large satellite footprint and rejection of complex waveforms [*Wingham et al.*, 2006]), as well as pressure ridges. It has been shown recently that the OIB radar system is impacted by ice surface morphology, and estimating snow depth uncertainty over heavily deformed sea ice remains challenging [*Newman et al.*, 2014]. Using a wavelet technique, *Newman et al.* [2014] found that snow radar-derived snow depths over MYI were larger than in the OIB Sea Ice Freeboard, Thickness, and Snow Depth product by 1 cm and 4 cm in 2011 and 2012, respectively. Similar differences in 2013–2014 would mean the radar penetration factors would be slightly smaller than in the analysis presented above.

Dedicated satellite underflights offer a solution to some of these issues. Having data collected directly under the satellite, with a time interval over which sea ice drift is not too large, solves the issue of time coincidence. It also allows a more detailed comparison of the two data sets through the availability of contemporary high resolution laser scans and photographs of the sea ice surface which allow the surface to be characterized in greater detail. As a general comment, we note that while comparisons between satellite and airborne data are crucial for sea ice freeboard/thickness evaluation, it is equally important to characterize the differences between measurement systems and bear these differences in mind when interpreting the results.

Leaving aside the caveats mentioned above and assuming that these results are a true representation of the Ka/Ku band dominant scattering horizons, we can calculate the impact that a value of $f < 1$ would have on the estimation of ice thickness for a given snow depth. Sea ice thickness is calculated from the ice freeboard as

$$h_i = \frac{\rho_s h_s + \rho_w F_i}{\rho_w - \rho_i} \tag{3}$$

where ρ_w, ρ_i and ρ_s are the densities of sea water, ice, and snow, respectively, and F_i is the ice freeboard. Conventionally, to estimate F_i, the factor $h_c = (1 - c_s/c)h_s$ is added to the radar freeboard to account for the reduced speed of propagation of radar waves through the snow pack. A value of $f < 1$ would affect the resulting estimate in two ways. First, the freeboard would be larger than the ice freeboard by $(1 - f)h_s$ due to the dominant scattering horizon lying above the ice-snow interface. Second, since the distance that the radar wave actually propagated through the snow layer is reduced by $(1 - f)h_s$, the freeboard would be larger again by a factor of $(1 - f)h_c$. The expression for the ice freeboard, accounting for the radar penetration, is then

$$F_i = F_r^{(\mathrm{sat})} - (1 - f)h_s + fh_c. \tag{4}$$

Inserting $f = 1$ into equation (4) (the sea ice surface is the dominant scattering horizon) gives $F_i = F_r^{(\mathrm{sat})} + h_c$, and inserting $f = 0$ (the snow surface is the dominant scattering horizon) gives $F_i = F_r^{(\mathrm{sat})} - h_s$, as expected.

For AltiKa, a value of $f = 0.46 \pm 0.05$ for all ice types means that if the radar penetration is not accounted for, the sea ice freeboard will be overestimated by $(0.66 \pm 0.06)h_s$. By inserting this into equation (3) we find that the thickness would be overestimated by $(4.75 \pm 0.43)h_s$ and $(6.31 \pm 0.57)h_s$ for MYI and FYI, respectively, where we use density values following *Giles et al.* [2007] and *Laxon et al.* [2013] and references therein that are representative of FYI and MYI in the Arctic. Clearly, radar penetration must be taken into account if AltiKa data were used to estimate sea ice thickness.

For CS2, a value of $f = 0.82 \pm 0.03$ over MYI leads to an overestimate of the ice freeboard by $(0.22 \pm 0.04)h_s$ if the radar penetration is not accounted for. This leads to an ice thickness overestimate of $(1.58 \pm 0.29)h_s$. By accounting for the radar penetration using equation (4) we can estimate the impact that using $f = 0.82$ rather than $f = 1$ has on Arctic MYI volume in March 2013 and 2014. The adjusted/unadjusted MYI volume is 4400/5700 km^3 for March 2013 and 7800/9700 km^3 for March 2014. The ice volume adjustment due to a value of $f < 1$ for CS2 over MYI could explain some of the observed differences between CS2 and Pan-Arctic Ice Ocean Modeling and Assimilation System (PIOMAS) observed by *Laxon et al.* [2013]. In reality, however,

the uncertainty due to the radar penetration is compounded with the uncertainty associated with using the climatological snow loading of *Warren et al.* [1999], and further work is need to unravel these uncertainties. We note also that the PIOMAS total sea ice volume uncertainty for March is 2250 km^3 and that PIOMAS also potentially underestimates the thickness of thick ice [*Schweiger et al.*, 2011].

5. Conclusions

It has been shown that it is possible to derive radar freeboard from AltiKa Ka band pulse-limited radar altimeter data. AltiKa consistently retrieves a larger elevation than CS2 over sea ice, ranging from 4.4 cm in October to 6.9 cm in March. The higher operating frequency of AltiKa makes the instrument more sensitive to scattering from the air-snow interface and/or the snow volume, which shifts the dominant scattering horizon toward the satellite resulting in a higher elevation retrieval than CS2. Through a comparison with OIB airborne laser freeboard and snow depth estimates it is shown that the AltiKa dominant scattering horizon lies $0.54h_s$ above the ice surface over all ice types in March. This would lead to an overestimate of the ice thickness of $4.75h_s$ and $6.31h_s$ for MYI and FYI, respectively, and must be accounted for if AltiKa is to be used for sea ice thickness calculations. While the CS2 elevation retrieval is consistent with ranging to the ice-snow interface over FYI, we find that the CS2 dominant scattering horizon lies, on average, $0.18h_s$ above the ice surface over MYI in March. This leads to MYI thickness overestimate of $1.58h_s$. While this could explain some of the observed difference between CS2 and PIOMAS reported by *Laxon et al.* [2013], the uncertainty due to radar penetration is currently not separable from the uncertainty associated with inadequate knowledge of the snow depth. Our results highlight both the need to consider radar penetration when estimating sea ice thickness and its uncertainty and the need for contemporary estimates of snow depth on Arctic sea ice.

Acknowledgments

Thanks to A. Shepherd for the assistance in preparing this manuscript for publication. This work was funded by a U.K. Natural Environment Research Council PhD studentship. AltiKa data were provided by CNES (ftp://avisoftp.cnes.fr/AVISO/pub/saral/); CS2 data were provided by the European Space Agency and processed by A. Ridout at the Centre for Polar Observation and Modelling, University College London, U.K.; sea ice concentration data were provided by the National Snow and Ice Data Center (http://nsidc.org/data/nsidc-0081); OIB data were provided by the National Snow and Ice Data Center (http://nsidc.org/data/icebridge/index.html); and sea ice type data were provided by the Ocean and Sea Ice Satellite Application Facility (http://osisaf.met.no/p/ice/).

The Editor thanks two anonymous reviewers for their assistance in evaluating this paper.

References

Armitage, T. W. K., and M. W. J. Davidson (2014), Using the interferometric capabilities of the ESA CryoSat-2 mission to improve the accuracy of sea ice freeboard retrievals, *IEEE Trans. Geosci. Remote Sens.*, *52*, 529–536, doi:10.1109/TGRS.2013.2242082.

Bronner, E. (2013), SARAL/AltiKa products handbook. Centre National d'Études Spatiales.

Connor, L. N., S. W. Laxon, A. L. Ridout, W. B. Krabill, and D. C. McAdoo (2009), Comparison of Envisat radar and airborne laser altimeter measurements over Arctic sea ice, *Remote Sens. Environ.*, *113*, 563–570, doi:10.1016/j.rse.2008.10.015.

Farrell, S. L., N. Kurtz, L. N. Connor, B. C. Elder, C. Leuschen, T. Markus, D. C. McAdoo, B. Panzer, J. Richter-Menge, and J. G. Sonntag (2012), A first assessment of IceBridge snow and ice thickness data over Arctic sea ice, *IEEE Trans. Geosci. Remote Sens.*, *50*, 2098–2111, doi:10.1109/TGRS.2011.2170843.

Giles, K. A., and S. M. Hvidegaard (2006), Comparison of space borne radar altimetry and airborne laser altimetry over sea ice in the Fram Strait, *Int. J. Remote Sens.*, *27*, 3105–3113, doi:10.1080/01431160600563273.

Giles, K. A., S. W. Laxon, D. J. Wingham, D. W. Wallis, W. B. Krabill, C. J. Leuschen, D. McAdoo, S. S. Manizade, and R. K. Raney (2007), Combined airborne laser and radar altimeter measurements over the Fram Strait in May 2002, *Remote Sens. Environ.*, *111*, 182–194, doi:10.1016/j.rse.2007.02.037.

Giles, K. A., S. W. Laxon, and A. L. Ridout (2008), Circumpolar thinning of Arctic sea ice following the 2007 record ice extent minimum, *Geophys. Res. Lett.*, *35*, doi:10.1029/2008GL035710.

Hendricks, S., L. Stenseng, V. Helm, and C. Haas (2010), Effects of surface roughness on sea ice freeboard retrieval with an airborne Ku-band SAR radar altimeter, paper presented at IEEE International Geoscience and Remote Sensing Symposium (IGARSS), held at Honolulu, Hawaii, pp. 3126–3129, doi:10.1109/IGARSS.2010.5654350, 25–30 July.

Kurtz, N. T., S. L. Farrell, M. Studinger, N. Galin, J. P. Harbeck, R. Lindsay, V. D. Onana, B. Panzer, and J. G. Sonntag (2013), Sea ice thickness, freeboard and snow depth products from Operation IceBridge airborne data, *Cryosphere*, *7*, 1035–1056, doi:10.5194/tc-7-1035-2013.

Kurtz, N. T., N. Galin, and M. Studinger (2014), An improved CryoSat-2 sea ice freeboard retrieval algorithm through the use of waveform fitting, *Cryosphere*, *8*, 1217–1237, doi:10.5194/tc-8-1217-2014.

Kwok, R. (2014), Simulated effects of a snow layer on retrieval of CryoSat-2 sea ice freeboard, *Geophys. Res. Lett.*, *41*, 5014–5020, doi:10.1002/2014GL060993.

Kwok, R., G. F. Cunningham, M. Wensnahan, I. Rigor, H. J. Zwally, and D. Yi (2009), Thinning and volume loss of the Arctic Ocean sea ice cover: 2003–2008, *J. Geophys. Res.*, *114*, C07005, doi:10.1029/2009JC005312.

Laxon, S. (1994), Sea ice altimeter processing scheme at the EODC, *Int. J. Remote Sens.*, *15*, 915–924, doi:10.1080/01431169408954124.

Laxon, S., N. Peacock, and D. Smith (2003), High interannual variability of sea ice thickness in the Arctic region, *Nature*, *425*, 947–950, doi:10.1038/nature02050.

Laxon, S. W., et al. (2013), CryoSat-2 estimates of Arctic sea ice thickness and volume, *Geophys. Res. Lett.*, *40*, 732–737, doi:10.1002/grl.50193.

Meier, W. N., et al. (2014), Arctic sea ice in transformation: A review of recent observed changes and impacts on biology and human activity, *Rev. Geophys.*, *52*, 185–217, doi:10.1002/2013RG000431.

Newman, T. N., S. L. Farrell, J. Richter-Menge, L. N. Connor, N. T. Kurtz, B. C. Elder, and D. McAdoo (2014), Assessment of radar-derived snow depth over Arctic sea ice, *J. Geophys. Res., Oceans*, *119*, 8578–8602, doi:10.1002/2014JC010284.

Onana, V., N. T. Kurtz, S. L. Farrell, L. S. Koenig, M. Studinger, and J. P. Harbeck (2013), A Sea-Ice lead detection algorithm for use with high-resolution airborne visible imagery, *IEEE Trans. Geosci. Remote Sens.*, *51*, 38–56, doi:10.1109/TGRS.2012.2202666.

Ricker, R., S. Hendricks, V. Helm, H. Skourup, and M. Davidson (2014), Sensitivity of CryoSat-2 Arctic sea-ice freeboard and thickness on radar-waveform interpretation, *Cryosphere*, *8*, 1607–1622, doi:10.5194/tc-8-1607-2014.

Ridout, A. L., and N. Ivanova (2012), Sea ice climate change initiative: Phase 1. Algorithm theoretical basis document, European Space Agency, v1.1. [Available at http://esa-cci.nersc.no/.]

Schweiger, A., R. Lindsay, J. Zhang, M. Steele, H. Stern, and R. Kwok (2011), Uncertainty in modelled arctic sea ice volume, *J. Geophys. Res.*, *116*, C00D06, doi:10.1029/2011JC007084.

Ulaby, F. T., R. K. Moore, and A. K. Fung (1986), *Microwave Remote Sensing: Active and Passive. Vol. 2: Radar Remote Sensing and Surface Scattering and Emission Theory*, pp. 848–851, Artech House, Norwood, Mass.

Warren, S. G., I. G. Rigor, N. Untersteiner, V. F. Radionov, N. N. Bryazgin, Y. I. Aleksandrov, and R. Colony (1999), Snow depth on Arctic sea ice, *J. Clim.*, *12*, 1814–1829, doi:10.1175/1520-0442(1999)012<1814:SDOASI>2.0.CO;2.

Willatt, R., S. Laxon, K. Giles, R. Cullen, C. Haas, and V. Helm (2011), Ku-band radar penetration into snow cover on the Arctic sea ice using airborne data, *Ann. Glaciol.*, *52*, 197–205, doi:10.3189/172756411795931589.

Willatt, R. C. (2012), Observations of radar penetration into snow on sea ice, PhD thesis, Univ. College London, Gower Street, London.

Wingham, D. J., et al. (2006), CryoSat: A mission to determine the fluctuations in Earth's land and marine ice fields, *Adv. Space Res.*, *37*, 841–871, doi:10.1016/j.asr.2005.07.027.